

**Dynamics of Sea Urchin Gastrulation Revealed by
Tracking Cells of Diverse Lineage and Regulatory State**

**Thesis by
Mat E. Barnet**

**In Partial Fulfillment of the Requirements
For the Degree of
Doctor of Philosophy in
Biochemistry & Molecular Biophysics**

**California Institute of Technology
Pasadena, CA
2011**

(Defended September 14, 2010)

© 2011

Mat E. Barnet

All Rights Reserved

Acknowledgments

First I would like to thank my advisor Scott Fraser for guidance over the past several years, and in particular his patience as I struggled through many failed attempts at immobilizing live sea urchin embryos. I would also like to thank Eric Davidson, especially for his guidance and insight once I could finally immobilize the embryos. Special thanks also to Dave McClay, with whom I worked closely while he visited Caltech on sabbatical, and whose eternal optimism that the next experiment would work flawlessly – even when the prior experiment was an abject failure – helped propel me through the experiments that comprise this thesis.

I want to thank my thesis committee for their assistance through this Ph.D. And the Fraser lab in general for creating a diverse scientific environment. Special thanks to Sean Megason, who, when I was extremely frustrated trying to figure out a mechanical way to immobilize sea urchin embryos, asked the question ‘Instead of restraining the embryos, is there a way to knock out their cilia to keep them from swimming?’ which, looking back, marked the turning point of my Ph.D. Additionally, from the Fraser lab I’ve received much advice about imaging, from Nico Plachta’s suggestion that I use a nucleary-localized fluorescent label to allow 4D imaging of embryos, to Bill Dempsey’s suggestion that I try a certain petri dish to eliminate an annoying z-drift, to discussions with Laki Pantazis about photoconvertible fluorescent proteins, and many other helpful pieces of advice from various people along the way. I have also received much advice about image processing from

Fraser lab members, chiefly from Willy Supatto, who was always willing to take time to help me with the program Imaris, and Michael Liebling, whose alignment plug-in for Imaris made tracking hundreds of cells feasible. I am also extremely grateful to Jen Yang, who in addition to providing advice about imaging and image processing, went through the Ph.D. process with me concurrently, just a few months ahead, and provided valuable insight into surviving it.

Members of the Davidson lab have also given valuable assistance during my Ph.D. Thanks to Sagar Damle for teaching me how to microinject sea urchin embryos, and for helping me troubleshoot failed injections later. To Andy Ransick for showing me his technique of constraining embryos in agar tunnels. To Andy Cameron and Smadar Ben-Tabou de-Leon for helpful discussions about the genes *brachyury* and *foxa*, respectively. To Isabelle Peter for extensive discussions about my time-lapse movies and the behavior of the endoderm. And special thanks to Julie Hahn for generating the recombineered BACs I used in my experiments, and for patiently leading me through the process of making them when I wanted to create a very nonstandard one.

Finally, I'd like to thank Mary Flowers, Martha Henderson, and Jane Rigg, for taking care of lots of the little things, and many of the bigger things as well.

Abstract

During gastrulation in the sea urchin embryo the archenteron, or primitive gut, is formed by an initial process of invagination at the vegetal pole of the embryo, followed by extension across the blastocoel toward the future mouth. Neither the genetic basis of gastrulation nor the detailed movement of the cells involved in archenteron formation is well understood. This thesis describes a new 4D imaging methodology by which embryonic lineage and gene regulatory states can be connected to cell behavior by tracking individual cells of the living embryo through developmental time. The work presented in this thesis shows directly the dramatic cellular rearrangement that comprises gastrulation. Furthermore, it shows that this rearrangement occurs in the veg2 lineage of cells expressing *foxa*, and not in the adjacent veg1 lineage of cells expressing *brachyury*. Very late in gastrulation some veg1 cells move in as a coherent truncated cone to produce the hindgut. However, veg1 cells located outside the vegetal ring of *brachyury* expression prior to gastrulation never contribute to the archenteron.

Table of Contents

Acknowledgments	iii
Abstract	v
Table of Contents	vi
Chapter 1: <i>Introduction</i>	1
Chapter 2: <i>Dynamics of Sea Urchin Gastrulation Revealed by Tracking Cells of Diverse Lineage and Regulatory State</i>	17
Chapter 3: <i>Conclusions</i>	52

Chapter 1: Introduction

The sea urchin embryo has been a favorite model organism of developmental biologists for more than a century. Reasons for this include that sea urchin embryos can be obtained in large numbers; they are fertilized externally and are easy to culture; exogenous genetic material is easy to introduce via microinjection; they are amenable to microsurgical transplantation of individual cells during their cleavage stages; and finally, the optical transparency of the embryo allows convenient study by light microscopy.

Because of its long history as a model organism for development, the sea urchin embryo has been extensively studied with respect to cell lineage¹. After fertilization, the embryo undergoes two holoblastic meridional cleavages (Fig. 1). The resulting four cells are identical in appearance, although it has been shown that the first cleavage plane acts as a reference for specification of the second embryonic axis, the oral-aboral axis² later in development. Third cleavage, which divides these four cells equatorially, produces two tiers of four cells each, with the cells arranged as the eight vertices of a cube. These eight cells also are identical in appearance, but have different fates depending on which of the two tiers they occupy, the so-called animal tier or the vegetal tier. Fourth cleavage gives rise to the first visible asymmetry in the embryo: the four animal tier blastomeres divide meridionally to produce eight mesomeres, while simultaneously the four vegetal tier blastomeres divide equatorially but unequally, producing four macromeres and four micromeres.

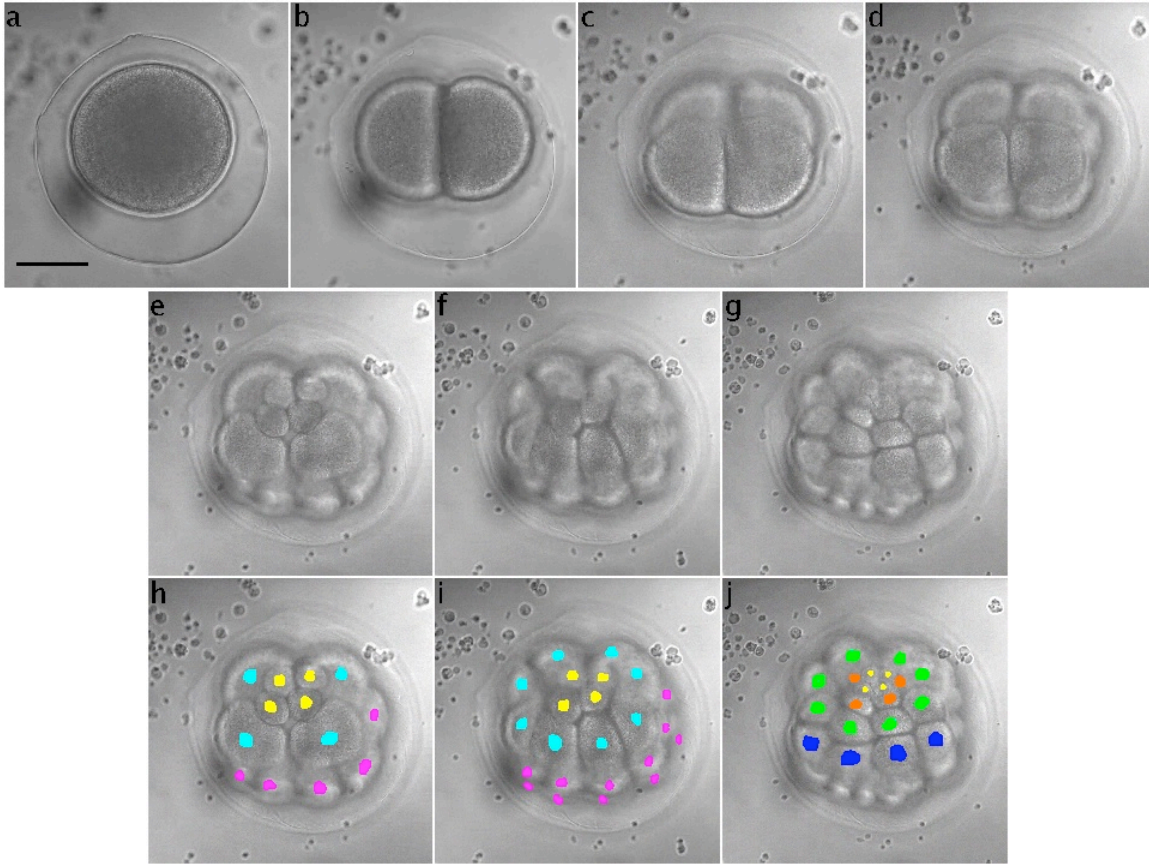


Figure 1 Cell lineages arising from the first six cleavages of the sea urchin embryo *Strongylocentrotus purpuratus*. **a**, fertilized egg. **b**, two-cell stage, resulting from first meridional cleavage. **c**, four-cell stage, resulting from second meridional cleavage. **d**, eight-cell stage, resulting from third equatorial cleavage. **e**, 16-cell stage, resulting from unequal equatorial cleavage of the four vegetal-tier blastomeres to form macromeres and micromeres, and meridional cleavage of the four animal-tier blastomeres to form mesomeres. **f**, 28-cell stage, resulting from meridional division of the macromeres and equatorial division of the mesomeres; in this species the micromeres do not divide until the macromeres and mesomeres are just about to undergo their next division. **g**, 56-cell stage, resulting from equatorial division of the macromere daughters, meridional division of the mesomere daughters, and unequal equatorial division of the micromeres. **h-j**, same images as e-g, but with cells color-coded by lineage. **h**, micromeres yellow, macromeres cyan, mesomeres magenta. **i**, micromeres yellow, macromere daughters cyan, mesomere daughters magenta. **j**, small micromeres yellow, large micromeres orange, veg2 cells green, veg1 cells blue. For simplicity, the animal-half blastomeres are not labeled in panel j. Scale bar 30 μm .

In some species, *Strongylocentrotus purpuratus* for example, the micromeres undergo subsequent divisions on a schedule different from the macromeres and mesomeres. Thus, fifth cleavage in *S. purpuratus* consists of a meridional division of the macromeres and an equatorial division of the mesomeres, as the micromeres remain undivided, resulting in a 28-cell embryo. The four micromeres undergo their first division, an unequal equatorial cleavage forming four small micromeres and four large micromeres, just before the eight macromere daughters and 16 mesomere daughters divide during sixth embryonic cleavage. The small micromeres will divide only once more during embryogenesis, to form eight cells. The large micromeres will divide either three or four more times, resulting in 32 or 64 progeny, depending on the species. Sixth cleavage results in 32 animal-half blastomeres derived from the mesomeres, and 16 vegetal-half blastomeres derived from the macromeres. These macromere descendants are arranged in two tiers each of eight cells; the tier bordering the mesomere descendants is called veg1, and the tier bordering the large micromeres is called veg2. The veg1, veg2, and animal-half blastomeres continue dividing, albeit in a less-synchronized and less-frequent manner, eventually forming an epithelial ball of cells, or blastula. During the ninth (asynchronous) cleavage cycle, the blastula hatches from its fertilization envelope (visible in Fig. 1) and begins to swim freely.

By the sixth-cleavage, 56-cell stage (or 60- or 64-cell stage, depending on whether the micromere division schedule matches the rest of the embryo in a given species), many of the founder lineages that generate the various domains in the later embryo have been established². Let us briefly survey each of these lineages.

Large micromere lineage

The large micromere lineage is perhaps conceptually the simplest place to begin, since cells of this lineage form only one type of tissue, the skeletogenic mesenchyme. Moreover, the skeletogenic mesenchyme arises exclusively from the large micromere lineage, with no contribution from other cell types of the sixth-cleavage embryo. Between the ninth cleavage cycle and the beginning of gastrulation, the cells of this lineage ingress from the epithelium of the vegetal plate into the blastocoel. After ingression, these cells lie on the vegetal end of the blastocoel, and form a syncytial ring consisting of 32 or 64 cells (depending on species) through which the archenteron will pass during gastrulation³. Later, this lineage produces the embryonic skeleton.

The specification of the skeletogenic mesenchyme is highly autonomous, as micromeres can be cultured *in vitro* to produce spicules characteristic of the *in vivo* embryonic skeleton^{4,5}. Furthermore, adding single micromeres ectopically to host embryos results in skeletogenic mesenchyme cells that ingress on schedule and join the host skeleton⁶. Additional support for autonomous specification of the skeletogenic mesenchyme lineage comes from experiments in which micromeres transplanted to the animal pole at the 16-cell stage induce the formation of a second skeleton and second gut⁷. (See below for more about the signaling implications of the second-gut result.)

The gene *pmar1* has been identified as a key regulator of micromere fate^{8,9}. *pmar1* operates via a double-negative logic gate, in which it represses *hesC*, itself a

repressor of other genes¹⁰. *pmar1* expression exclusively in the micromere lineage prevents expression of *hesC*, which is otherwise ubiquitously expressed in the embryo. *hesC* represses skeletogenic regulatory factors such as *tbrain*, *ets1*, and *delta*; thus its repression by *pmar1* allows the expression of these factors exclusively in the micromere lineage, driving its specification¹¹.

Small micromere lineage

As mentioned above, the small micromeres arise from the unequal cleavage of the four micromeres, which themselves had arisen from the unequal fourth cleavage. The four small micromere founders divide only once more during embryogenesis, resulting in an eight-cell lineage^{12,13}. In the early blastula-stage embryo, prior to ingression of the skeletogenic mesenchyme, the small micromeres are located at the embryonic vegetal pole. The large micromere descendants, which will become the skeletogenic mesenchyme, surround the small micromeres in the epithelium of the vegetal plate. During ingression, skeletogenic mesenchyme cells move individually out of the vegetal plate and into the blastocoel, while the small micromeres remain in the vegetal plate¹⁴. It is not well understood how the small micromeres remain epithelial while the ring of cells surrounding them becomes mesenchymal. After ingression of the skeletogenic mesenchyme, the small micromeres are surrounded by cells of the *veg2* lineage fated to become non-skeletogenic mesoderm¹⁵. Later, during gastrulation, the small micromeres will be carried along with a subset of these *veg2* mesodermal cells near the tip of the forming archenteron, joining them in forming the coelomic pouches. As far as is

known, the small micromeres are essentially set aside in this manner during embryogenesis, only to give rise to mesodermal structures of the adult¹⁶.

Veg2 lineage

Cells of the veg2 lineage contribute to both non-skeletogenic mesoderm (NSM) and endoderm tissue. The non-skeletogenic mesoderm consists of four cell types: pigment cells, which insert into the ectoderm^{17,18}; blastocoelar cells, which have an immune function¹⁹; coelomic pouch cells (mentioned above); and muscle cells that encircle the foregut²⁰. During gastrulation, NSM cells at the tip of the forming archenteron extend filopodia into the blastocoel. It was originally thought that these filopodia contributed to the extension of the archenteron by pulling it toward the stomodeum, or future mouth²¹. More recently, however, the amount of this contribution has been revised downward, although functional mesodermal cells still appear to be required during the late stage of archenteron elongation, if nothing else to guide the archenteron to the stomodeum²².

Signaling from the micromere descendants to cells of the veg2 lineage is crucial for veg2 mesodermal specification. Two such signaling events occur during cleavage. First, during fourth to fifth cleavage, a signal (the identity of which remains unknown) is required for proper specification of endomesoderm²³. Moreover, the ectopic placement of micromeres near presumptive ectoderm alters its fate to endomesodermal⁷. Second, during the interval of eighth to ninth cleavage, prior to their ingression large micromere descendants express the Delta ligand, which activates a Notch receptor in adjacent veg2 progeny. This event is required for

specification of these veg2 cells as mesoderm²⁴⁻²⁷. Veg2 progeny not in immediate contact with the large micromere descendants do not participate in this Delta-Notch signaling, and thus do not become mesoderm, instead becoming endoderm.

For a long time, the veg2 lineage was thought to be the only contributor to endodermal tissue in the sea urchin embryo¹. More recently, detailed fate-mapping to late embryonic stages showed that cells from the veg1 lineage contribute to the hindgut late in gastrulation, and even to the midgut by prism stage^{28,29}. Prior studies on the mechanics of gastrulation tended to focus on the earlier phases of gastrulation, so their conclusions are largely drawn from the behavior of veg2-derived cells. For example, Ettensohn showed that the mechanical forces involved in gastrulation are generated within the vegetal plate, since isolated vegetal plates were observed to undergo invagination³⁰. Ettensohn also deduced that cells of the elongating archenteron undergo rearrangement, by noting that the number of cells in cross sections of archenterons of older embryos was less than that of younger embryos³¹. Until this thesis, however, the only direct observation of cellular rearrangement during gastrulation was in the cidaroid urchin, *Eucidaris tribuloides*³². Unfortunately this observation spanned a relatively short period of gastrulation. Additionally, *E. tribuloides*, a cidaroid urchin, is known to differ morphogenetically from euechinoid urchins, at least in regard to the behavior of the skeletogenic mesenchyme: in *E. tribuloides*, ingression of this lineage is not precocious, instead occurring as part of gastrulation. The main impetus of this thesis was to investigate cellular movement during the entirety of gastrulation, and in a euechinoid urchin. In addition to cellular movement, cell division was investigated, since inhibition of DNA

synthesis and subsequent mitosis has been shown to block gastrulation in one species, *Lytechinus variegatus*³³, but not in another, *Lytechinus pictus*³⁴.

Recent evidence suggests that prior to hatching stage (eighth – ninth cleavage) cells of the entire veg2 lineage exist in a regulatory state characteristic of endoderm³⁵. At this time, endodermal transcription factors such as *foxa*, *blimp1*, and *hox11/13* are expressed throughout the lineage. As mentioned briefly above, subsequent differentiation of the veg2-derived mesoderm from the veg2-derived endoderm is a result of Delta-Notch signaling from the large micromere descendants to the immediately adjacent ring of veg2 cells. Expression of *gcm*, a direct target of Notch³⁶, is maintained in this ring of veg2 cells, leading to their specification as mesoderm. Expression of *gcm* in veg2 cells peripheral to this ring wanes, due to their lack of direct contact with the Delta-expressing large micromere descendants, and these cells maintain their endodermal specification³⁵.

Veg1 lineage

As mentioned above, until fairly recently the veg1 lineage was thought to specify exclusively ectoderm. The discovery of a veg1 contribution to endoderm implied a later specification of this lineage than had been assumed^{28,29}. The veg1 endoderm shares a set of regulatory genes with the veg2 endoderm, notably *brachyury* and *endo16*, although expression of the latter in veg1 lags its expression in veg2²⁹. Interestingly, *brachyury* is initially expressed in the veg2 lineage, then later only in the veg1 lineage, and is thought to play a role in defining the endoderm-ectoderm boundary³⁷. Unfortunately, gene network analysis of the veg1 lineage is

not yet as mature as for the *veg2* or large micromere lineages. Nonetheless, the spatial and temporal expression of *brachyury* will be thoroughly explored in this thesis.

Lineages of the animal half of the embryo

The animal-half lineages are outside the scope of this work. It suffices to say that they specify exclusively ectoderm, that morphologically this ectoderm extends somewhat vegetally during gastrulation³⁸, and that their governing gene regulatory network is an emerging area of research³⁹.

Goal of thesis

In this thesis, I explore the relationships among lineage, regulatory state, and morphogenetic behavior of the cells that form the endoderm of the sea urchin embryo.

References

- 1 Hardin, J. The cellular basis of sea urchin gastrulation. *Curr Top Dev Biol* **33**, 159-262 (1996).
- 2 Cameron, R. A. & Davidson, E. H. Cell type specification during sea urchin development. *Trends Genet* **7**, 212-218 (1991).
- 3 Etensohn, C. A. Cell interactions and mesodermal cell fates in the sea urchin embryo. *Dev Suppl*, 43-51 (1992).
- 4 Okazaki, K. Spicule Formation by Isolated Micromeres of Sea-Urchin Embryo. *Am Zool* **15**, 567-581 (1975).
- 5 Wilt, F. H. Determination and morphogenesis in the sea urchin embryo. *Development* **100**, 559-576 (1987).
- 6 Wray, G. A. & McClay, D. R. The origin of spicule-forming cells in a 'primitive' sea urchin (*Eucidaris tribuloides*) which appears to lack primary mesenchyme cells. *Development* **103**, 305-315 (1988).
- 7 Ransick, A. & Davidson, E. H. A Complete 2nd Gut Induced by Transplanted Micromeres in the Sea-Urchin Embryo. *Science* **259**, 1134-1138 (1993).

- 8 Oliveri, P., Carrick, D. M. & Davidson, E. H. A regulatory gene network that directs micromere specification in the sea urchin embryo. *Developmental Biology* **246**, 209-228, doi:Doi 10.1006/Dbio.2002.0627 (2002).
- 9 Oliveri, P., Davidson, E. H. & McClay, D. R. Activation of pmar1 controls specification of micromeres in the sea urchin embryo. *Developmental Biology* **258**, 32-43, doi:Doi 10.1016/S0012-1606(03)00108-8 (2003).
- 10 Revilla-I-Domingo, R., Oliveri, P. & Davidson, E. H. A missing link in the sea urchin embryo gene regulatory network: hesC and the double-negative specification of micromeres. *Proceedings Of The National Academy Of Sciences Of The United States Of America* **104**, 12383-12388, doi:Doi 10.1073/Pnas.0705324104 (2007).
- 11 Oliveri, P., Tu, Q. & Davidson, E. H. Global regulatory logic for specification of an embryonic cell lineage. *Proceedings Of The National Academy Of Sciences Of The United States Of America* **105**, 5955-5962, doi:Doi 10.1073/Pnas.0711220105 (2008).
- 12 Pehrson, J. R. & Cohen, L. H. The fate of the small micromeres in sea urchin development. *Dev Biol* **113**, 522-526, doi:0012-1606(86)90188-0 [pii] (1986).

- 13 Davidson, E. H., Cameron, R. A. & Ransick, A. Specification of cell fate in the sea urchin embryo: summary and some proposed mechanisms. *Development* **125**, 3269-3290 (1998).
- 14 Amemiya, S. Electron microscopic studies on primary mesenchyme cell ingression and gastrulation in relation to vegetal pole cell behavior in sea urchin embryos. *Exp Cell Res* **183**, 453-462 (1989).
- 15 Ruffins, S. W. & Etensohn, C. A. A fate map of the vegetal plate of the sea urchin (*Lytechinus variegatus*) mesenchyme blastula. *Development* **122**, 253-263 (1996).
- 16 Peterson, K. J., Cameron, R. A. & Davidson, E. H. Set-aside cells in maximal indirect development: evolutionary and developmental significance. *Bioessays* **19**, 623-631, doi:10.1002/bies.950190713 (1997).
- 17 Gibson, A. W. & Burke, R. D. The Origin of Pigment-Cells in Embryos of the Sea-Urchin *Strongylocentrotus-Purpuratus*. *Developmental Biology* **107**, 414-419 (1985).
- 18 Etensohn, C. A. & McClay, D. R. The Regulation of Primary Mesenchyme Cell-Migration in the Sea-Urchin Embryo - Transplantations of Cells and Latex Beads. *Developmental Biology* **117**, 380-391 (1986).

- 19 Stevens, M. E. *et al.* SpTie1/2 is expressed in coelomocytes, axial organ and embryos of the sea urchin *Strongylocentrotus purpuratus*, and is an orthologue of vertebrate Tiel and Tie2. *Dev Comp Immunol* **34**, 884-895, doi:Doi 10.1016/J.Dci.2010.03.010 (2010).
- 20 Wessel, G. M., Zhang, W. & Klein, W. H. Myosin Heavy-Chain Accumulates in Dissimilar Cell-Types of the Macromere Lineage in the Sea-Urchin Embryo. *Developmental Biology* **140**, 447-454 (1990).
- 21 Dan, K. & Okazaki, K. Cyto-Embryological Studies of Sea Urchins .3. Role of the Secondary Mesenchyme Cells in the Formation of the Primitive Gut in Sea Urchin Larvae. *Biol Bull* **110**, 29-42 (1956).
- 22 Hardin, J. The Role of Secondary Mesenchyme Cells during Sea-Urchin Gastrulation Studied by Laser Ablation. *Development* **103**, 317-324 (1988).
- 23 Ransick, A. & Davidson, E. H. Micromeres Are Required for Normal Vegetal Plate Specification in Sea-Urchin Embryos. *Development* **121**, 3215-3222 (1995).
- 24 Sherwood, D. R. & McClay, D. R. LvNotch signaling mediates secondary mesenchyme specification in the sea urchin embryo. *Development* **126**, 1703-1713 (1999).

- 25 Sherwood, D. R. & McClay, D. R. LvNotch signaling plays a dual role in regulating the position of the ectoderm-endoderm boundary in the sea urchin embryo. *Development* **128**, 2221-2232 (2001).
- 26 McClay, D. R., Peterson, R. E., Range, R. C., Winter-Vann, A. M. & Ferkowicz, M. J. A micromere induction signal is activated by beta-catenin and acts through Notch to initiate specification of secondary mesenchyme cells in the sea urchin embryo. *Development* **127**, 5113-5122 (2000).
- 27 Sweet, H. C., Hodor, P. G. & Etensohn, C. A. The role of micromere signaling in Notch activation and mesoderm specification during sea urchin embryogenesis. *Development* **126**, 5255-5265 (1999).
- 28 Logan, C. Y. & McClay, D. R. The allocation of early blastomeres to the ectoderm and endoderm is variable in the sea urchin embryo. *Development* **124**, 2213-2223 (1997).
- 29 Ransick, A. & Davidson, E. H. Late specification of veg(1) lineages to endodermal fate in the sea urchin embryo. *Developmental Biology* **195**, 38-48 (1998).
- 30 Etensohn, C. A. Primary Invagination of the Vegetal Plate during Sea-Urchin Gastrulation. *Am Zool* **24**, 571-588 (1984).

- 31 Ettensohn, C. A. Gastrulation in the Sea-Urchin Embryo Is Accompanied by the Rearrangement of Invaginating Epithelial-Cells. *Developmental Biology* **112**, 383-390 (1985).
- 32 Hardin, J. Local Shifts in Position and Polarized Motility Drive Cell Rearrangement during Sea-Urchin Gastrulation. *Developmental Biology* **136**, 430-445 (1989).
- 33 Nislow, C. & Morrill, J. B. Regionalized Cell-Division during Sea-Urchin Gastrulation Contributes to Archenteron Formation and Is Correlated with the Establishment of Larval Symmetry. *Development Growth & Differentiation* **30**, 483-499 (1988).
- 34 Stephens, L., Hardin, J., Keller, R. & Wilt, F. The Effects of Aphidicolin on Morphogenesis and Differentiation in the Sea-Urchin Embryo. *Developmental Biology* **118**, 64-69 (1986).
- 35 Peter, I. S. & Davidson, E. H. The endoderm gene regulatory network in sea urchin embryos up to mid-blastula stage. *Developmental Biology* **340**, 188-199, doi:Doi 10.1016/J.Ydbio.2009.10.037 (2010).
- 36 Ransick, A. & Davidson, E. H. cis-regulatory processing of Notch signaling input to the sea urchin glial cells missing gene during mesoderm specification. *Dev Biol* **297**, 587-602, doi:S0012-1606(06)00876-1 [pii]

10.1016/j.ydbio.2006.05.037 (2006).

- 37 Gross, J. M. & McClay, D. R. The role of Brachyury (T) during gastrulation movements in the sea urchin *Lytechinus variegatus*. *Developmental Biology* **239**, 132-147 (2001).
- 38 Burke, R. D., Myers, R. L., Sexton, T. L. & Jackson, C. Cell Movements during the Initial Phase of Gastrulation in the Sea-Urchin Embryo. *Developmental Biology* **146**, 542-557 (1991).
- 39 Su, Y. H. *et al.* A perturbation model of the gene regulatory network for oral and aboral ectoderm specification in the sea urchin embryo. *Developmental Biology* **329**, 410-421, doi:Doi 10.1016/J.Ydbio.2009.02.029 (2009).

Chapter 2

Dynamics of sea urchin gastrulation revealed by tracking cells of diverse lineage and regulatory state

Mat E. Barnet, Isabelle S. Peter, Eric H. Davidson & Scott E. Fraser

Submitted for publication to *Nature Cell Biology*

During gastrulation in the sea urchin embryo the archenteron, or primitive gut, is formed by an initial process of invagination at the vegetal pole of the embryo, followed by extension across the blastocoel toward the future mouth. Neither the genetic basis of gastrulation nor the detailed movement of the cells involved in archenteron formation is well understood. We developed a 4D imaging methodology by which embryonic lineage and gene regulatory states can be connected to cell behavior by tracking individual cells of the living embryo through developmental time. Here we show directly the dramatic cellular rearrangement that comprises gastrulation. We found that this rearrangement occurs in the veg2 lineage of cells expressing *foxa*, and not in the adjacent veg1 lineage of cells expressing *brachyury*. Very late in gastrulation some veg1 cells move in as a coherent truncated cone to produce the hindgut. However, veg1 cells located outside the vegetal ring of *brachyury* expression prior to gastrulation never contribute to the archenteron.

Though the cellular basis of gastrulation in sea urchin embryos has long been studied¹⁻⁴, many aspects of the mechanism remain obscure or controversial, even including the exact identity of the pregastrular cells that will form the archenteron. In *Strongylocentrotus purpuratus*, gastrulation begins about 30 hours post fertilization (hpf). The cleavage stage embryo undergoes stereotyped cleavages, generating an embryo with clearly defined animal-vegetal polarity (Fig. 1a), which by 30 hpf has undergone further cleavages and morphogenetic movements to generate the late blastula. Morphologically, at 30 hpf the embryo consists of a hollow epithelial ball within which lie 32 skeletogenic mesenchyme cells, the progenitors of which had ingressed into the blastocoel 8-9 hours earlier (Fig. 1b). These cells are positioned at one end of the blastocoel, overlying the concentrically arranged territories of the vegetal plate that will ultimately generate the archenteron (Fig. 1e). In the center of the vegetal plate is the non-skeletogenic mesoderm territory, and surrounding this is a torus of ~60-64 future anterior endoderm cells. Both of these territories descend from the sixth cleavage veg2 lineage (Fig. 1a). Immediately adjacent is a peripheral torus consisting of ~60-64 future posterior endoderm cells, descendant from the sixth cleavage veg1 lineage, surrounded in turn by future ectoderm cells, also of veg1 descent. By well before gastrulation each of these territories has come to express an exclusive regulatory state, i.e., a specific set of transcription factors⁵. Those regulatory genes with which we are here concerned are *foxa*, a member of the anterior veg2 endoderm gene regulatory network; and *brachyury*, similarly a canonical member of the veg1 endoderm gene regulatory network. A representative double in situ hybridization showing the adjacent and exclusive expression of the

endogenous *foxa* and *brachyury* genes is shown in Fig. 1d. Expression of these and many other genes contributing to the endodermal regulatory states is required for gastrulation to occur⁶⁻⁸. A small GTPase, RhoA, has also been implicated in gastrulation, regulating the initial invagination of the vegetal plate, but not the later extension of the archenteron⁹. While our understanding of the pregastrular specification molecular biology of the endomesodermal territories is rapidly improving¹⁰, a comprehensive view of gastrulation linking gene regulatory state to lineage and cell behavior remains elusive, in part because of the difficulty of dynamically assaying cell behavior.

Although the optical transparency of the embryo permits convenient study by light microscopy, its continuous swimming motion following hatching (after the ninth cleavage cycle; ~18 hpf) makes direct observation of gastrulation challenging (see Supplementary Information, Video S1 online). Fixation of embryos allows for snapshots of gene expression¹¹ and fine structural detail¹², but precludes examination of individual embryos at multiple stages of development. Imaging of live embryos in previous studies has typically been confined to following individual cells for relatively short periods of development¹³, or observing clonal populations of cells for longer periods¹⁴⁻¹⁶. But since individual cells have so far not been tracked over long periods of development, the detailed cellular movements driving gastrulation have not been clarified. One hypothesis is that cells originating peripherally to the blastopore ‘tractor’ through the blastoporal ring to supply material for the forming archenteron^{2,15-17}. A competing hypothesis is that archenteron growth is driven entirely by cell shape change and rearrangement^{18,19}, without the addition of cells

from outside the blastopore¹³. It also remains unclear to what extent cell division contributes to archenteron growth, since in at least one species gastrulation can proceed in the absence of DNA synthesis and cell division²⁰. Relating this morphogenetic phenomenology to the underlying regulatory states of the cells, in the living embryo, presents a key experimental challenge.

RESULTS

In vivo time-lapse imaging of gene expression

To directly assay morphogenesis in the context of gene regulatory state and lineage, we developed a method that would permit immobilization and imaging of individual living sea urchin embryos for many hours. Its basis is the injection into fertilized eggs of an antibody that recognizes the heterotrimeric kinesin-2 motor protein, which results in the growth of immotile cilia²¹. The embryos do not swim but otherwise develop normally through to the earliest feeding stages (pluteus); however, the effect of this antibody on later-stage neural function has not been studied in the sea urchin, and blocking the kinesin-2 motor protein complex in mouse has been shown to block neurite outgrowth²². By coinjecting recombiner DNA reporters with the antibody, we can follow the expression of specific genes over time. Here we use this method to follow for many hours the expression of *foxa* and *brachyury* (Fig. 1f; Supplementary Information, Video S2 online). Expression assayed by these fluorescent protein reporters is consistent with mRNA expression assayed by whole-mount *in situ* hybridization (WMISH)^{5,8,23,24}. At mesenchyme blastula stage (24 hpf, Fig. 1b), *brachyury* is expressed in a ring of veg1 cells and

foxa is expressed inside of this ring, in the veg2 endoderm cells of the vegetal plate (Fig. 1d). Later, during gastrulation, *foxa* is expressed in the forming archenteron, while *brachyury* expression continues in the blastoporal ring at the base of the archenteron.

The results of the BAC-reporter and WMISH assays are visually non-identical in two respects. Spatially, the BAC expression is mosaic and is observed in only a portion of the endogenous expression domain because the exogenous DNA incorporates into the genome only after the first, second, or third embryonic cleavage²⁵. Temporally, there is a delay between mRNA transcription detected by WMISH and the translation, folding, fluorescence maturation, and accumulation of fluorescent protein sufficient for microscopic detection. Additionally, fluorescent protein expression can perdure for several hours after transcription of the reporter has turned off, due to stability of the fluorescent protein. Thus we observe in Figure 1f mesodermal cells continuing to fluoresce red after *foxa* transcription has stopped in these cells, and veg2-derived cells continuing to fluoresce green after *brachyury* transcription has ceased in them. Keeping these caveats in mind, the time-lapse technique allows us to monitor the regulatory states of individual cells in living embryos as they develop.

Cells outside the vegetal ring of brachyury expression prior to gastrulation do not contribute to the archenteron, or to the blastopore, during gastrulation

To connect the regulatory state of individual cells to their behavior, we labeled all of the nuclei in the embryo by injecting mRNA that encodes a nuclear-targeted

fluorescent protein, H2B-mCherry. Coinjecting this mRNA, together with a *brachyury:GFP* BAC reporter and anti-kinesin-2 antibody, facilitated confocal time-lapse microscopy during gastrulation, and thus allowed us to track the trajectory of any individual cell.

By tracking cells outside the vegetal ring of *brachyury* expression prior to gastrulation, we observed that these cells do not contribute to the archenteron, or to the blastopore, during gastrulation (Fig. 2; Supplementary Information, Videos S3-S6 online). They remain in an almost fixed position, external to the blastopore throughout. Nor do cells originating outside the blastopore ever turn on *brachyury* expression, even if they move by one or two cell diameters toward the vegetal pole. Because *Strongylocentrotus purpuratus* gastrulates asymmetrically, with a distinct oral-aboral bias, we evaluated both aboral (Fig. 2a-b) and oral (Fig. 2c-d) *brachyury:GFP* BAC clones, and found the same result. Since some progeny of veg1 cells are known to contribute to the hindgut late in gastrulation^{14,16}, we performed the same experiment, but imaging at later developmental stages, to determine whether cells outside the *brachyury* ring would ever contribute to the archenteron (Fig. 3; Supplementary Information, Videos S7-S8 online). We find that even as late as prism stage, such cells neither contribute to the archenteron nor to the blastopore. Interestingly, by this later stage several of the cells that had initially expressed the *brachyury* reporter were no longer GFP-positive, suggesting they had turned off *brachyury* expression some hours earlier. This is consistent with WMISH data showing early expression of *brachyury* first in the veg2 lineage^{5,24} but later pregastrular expression only in the veg1 lineage^{8,11}. The midgut cells that turn off

brachyury in our time lapses are likely veg2-derived. Together, these results show that the fixed location of the *brachyury* ring during gastrulation¹¹ is due to the relatively fixed location of veg1 cells expressing this gene. We find no evidence to support the hypothesis of a highly dynamic regulatory situation in which cells tractor into the ring of *brachyury* expression, turn on *brachyury* themselves, and thence enter the archenteron.

Veg2 cells expressing *foxa* create the anterior endoderm by intercalative convergent extension, whereas veg1 cells expressing *brachyury* coherently form the hindgut and blastopore

If the cells that form the archenteron do not originate outside the ring of *brachyury* expression, then they must arise from the cells of the ring and/or inside the ring, possibly by means of cellular rearrangement. Cellular rearrangement has been deduced in a euechinoid sea urchin¹⁸, but has been directly observed only during a brief period of gastrulation in the cidaroid sea urchin, *Eucidaris tribuloides*¹³. To observe the movements of individual cells, we injected the *foxa* BAC, which is expressed during gastrulation in cells of the veg2-derived anterior endoderm²³, and followed the trajectories of five such cells during gastrulation. This experiment provided incontrovertible evidence of significant rearrangement (Fig. 4; Supplementary Information, Videos S9-S10 online). Thus within the *foxa* expression domain, the localization of cells in the pregastrular embryo does not relate to position within the growing archenteron, e.g., the distal blue cell in Fig. 4 ends up most anterior in the forming gut. Thus the veg2 regulatory state imposes a type of

cell behavior such that the positions of the individual cells are not defined but the position of the domain is.

To connect the morphogenetic movements of cells directly to their lineages, we performed a time lapse spanning 49 hours of development, from the ninth-cleavage blastula stage (15 hpf) to prism stage (64 hpf), and tracked the nuclei of cells at different positions in the vegetal plate (Fig. 5; Supplementary Information, Videos S11-S14 online). Viewing the sea urchin embryo from the vegetal pole at ninth cleavage, the various lineages are arranged in concentric rings^{5,26}. The skeletogenic mesenchyme cells were easily identified in our time lapse sequence by their precocious ingression. The veg2 non-skeletogenic mesoderm cells, which surround the skeletogenic mesenchyme cells in the vegetal plate prior to their ingression, could be identified by their epithelial-mesenchymal transition during gastrulation. The next lineages, radially outward from the vegetal pole, are the veg2 endoderm, followed by veg1. To assign the pregastrular veg1/veg2 boundary at the start of our 49-hour time lapse, we utilized a different time lapse, spanning sixth through ninth cleavage stages (Fig. 6; Supplementary Information, Videos S15-S16 online). In this early-stage time lapse, the cells comprising the vegetal half of the sixth cleavage embryo (56-cell stage) were identified (four small micromeres, four large micromeres, eight veg2 and eight veg1 cells). Tracking the division of these cells through seventh, eighth, and ninth cleavages revealed the veg1 and veg2 progeny at the time in development corresponding to the start of the 49-hour time lapse. At this time, approximately 64 veg2 progeny (non-skeletogenic mesoderm plus veg2 endoderm) form a concentric ring around the skeletogenic mesenchyme

cells, and 64 veg1 progeny surround the veg2 ring. Thus, by assigning to the veg2 lineage approximately 64 cells surrounding the skeletogenic mesenchyme cells at the beginning of the 49-hour time lapse, we identified a reasonably accurate boundary between the veg1 and veg2 lineages.

The time lapse sequence shows that the archenteron forms primarily from veg2-derived cells, with contributions to the blastopore and hindgut from the veg1 lineage late in gastrulation (Fig. 5; Supplementary Information, Videos S11-S14 online). This result is consistent with previous fate-mapping experiments^{14,16}. The general ordering of lineages is maintained, i.e., the veg2 lineage forms the anterior endoderm while the veg1 lineage contributes to the posterior endoderm. To examine the ordering in more detail, we computationally color-coded cells into four groups along the length of the archenteron at the end of the time lapse, then performed a 'reverse fate-mapping' to see where these cells originated (Fig. 7; Supplementary Information, Videos S17-S19 online). We found that the ordering of concentric rings of cells is remarkably maintained during gastrulation, albeit with some local mixing. Color-coding the cells circumferentially instead of radially showed the same general maintenance of ordering, again with some local mixing (Fig. 8; Supplementary Information, Videos S20-S21 online). To look more closely at the local mixing, we color-coded the same veg1 and veg2 cells more finely, in six radial stripes spanning one-quarter the circumference of the embryo (Fig. 9; Supplementary Information, Videos S22-S25 online). During gastrulation the veg2 cells dramatically rearranged by mediolateral intercalation. For example, some cells that had been separated by four to five cells prior to gastrulation became neighbors by the end of gastrulation

(convergence). Other cells that had been neighbors prior to gastrulation became separated by four to five cells by the end (extension). This type of rearrangement occurred only in the veg2 lineage (Fig. 9c; Supplementary Information, Video S24 online). In direct contrast, cells of the veg1 lineage (Fig. 9d; Supplementary Information, Video S25 online) changed position little as they formed the blastopore and hindgut. Neighboring cells moved as coherent groups as they formed the continuous low truncated cone of the hindgut.

As all of the cells were labeled by the injection of mRNA for H2B-mCherry, the time lapse sequences permitted us to assess the potential role of mitosis as a driving force of archenteron elongation. Between ninth cleavage and the beginning of gastrulation, most veg1 and veg2 cells divide once; in contrast, only nine of 52 tracked veg2 endodermal cells and only nine of 63 tracked veg1 cells divided during the 29-hour period encompassing gastrulation. Thus, cell rearrangement by convergence and extension, rather than cell division, must be a primary driver of archenteron elongation.

DISCUSSION

We have shown directly the cellular rearrangement that comprises gastrulation in the sea urchin embryo. This phenomenon is ultimately driven by gene regulatory networks (GRNs) operating within the cells involved²⁷. The striking difference between the intercalative convergent extension of veg2-derived cells, and the relative non-rearrangement of veg1-derived cells, suggests that the *foxa* regulatory state operating in the veg2 endodermal precursors and the *brachyury*

regulatory state operating in the veg1 endodermal precursors drive dramatically different morphogenetic programs. Our data support a model of gastrulation (Fig. 10) such that the different morphogenetic behavior of veg1 endoderm and veg2 endoderm cells in gastrulation is a direct consequence of the pregastrular expression of different regulatory states in these two lineages. The *foxa* regulatory state in cells of the veg2 endoderm causes them to rearrange by intercalation, thus driving elongation of the archenteron, whereas the *brachyury* regulatory state in cells of the veg1 lineage prevents them from substantial rearrangement. The prediction follows that there will be significantly diverse sets of cytoskeletal and motility genes expressed in these two endoderm lineages. The ring of veg1 cells actively expressing *brachyury* appears to remain static because it is in fact static, i.e., these cells do not move individually by more than one or two cell diameters. Eventually, the inner portion of the blastoporal torus is tipped or drawn inward, coherently forming the hindgut. Although our assay is not highly sensitive to protein turnover (we note veg2 cells losing GFP fluorescence, but due to the stability of GFP we cannot say how many hours earlier transcriptional expression had ceased), we can easily observe expression coming on. Since cells outside the ring of *brachyury* expression prior to gastrulation do not turn on *brachyury* during gastrulation, we conclude that tractoring of cells through the ring does not occur. In our model, the veg1 cells that contribute to the archenteron late in gastrulation do so as a coherent epithelial cone, with little rearrangement; and they originate inside rather than outside the *brachyury* ring of the mesenchyme blastula embryo.

We anticipate our time-lapse technique to be a starting point for studies linking embryonic GRNs to downstream, lineage-specific morphogenetic functions. By using fast-folding and fast-decaying fluorescent proteins as gene reporters, gene expression dynamics could be measured with greater temporal resolution than in the current study. Application of membrane-targeted fluorescent proteins would enable measurement of cell shape change and characterization of the roles of given downstream proteins in morphogenesis. Comparisons of detailed morphogenetic behavior across different species of sea urchin would also be fruitful. As many subtle differences have been reported to exist^{13,14,16}, this would suggest that in the course of evolution different downstream effector genes might have been wired into the gastrular specification GRNs.

METHODS

Antibody preparation

Kinesin II Monoclonal Antibody (catalog #MMS-198P) was obtained from Covance. Upon initial thawing, it was concentrated eight-fold (from 1 mg/ml to 8 mg/ml) using a Microcon YM-50 Centrifugal Filter Unit (Millipore catalog #42423), resuspending in PBS. Aliquots were stored at -20 °C.

Sea urchin embryos and microinjection

Strongylocentrotus purpuratus gametes were prepared for microinjection as described²⁸. For experiments involving BAC DNA, antibody, and mRNA injection, combination into a single cocktail often resulted in lack of expression of injected mRNA. Thus two separate injections were performed sequentially on each fertilized egg, the first consisting of BAC plus mRNA (5.0 µl injection solution: ~100 ng BAC, ~1 µg mRNA, 120 mM KCl), the second consisting of antibody (5.0 µl injection solution: ~25 µg concentrated antibody, 120 mM KCl). All injection solutions were centrifuged at 13000 rpm for six minutes, then transferred to a fresh tube to remove potential needle-clogging debris, prior to loading into injection needles.

Injections were performed using a picospritzer with air pressure regulated to 40 psig. Each pulse was 5-50 milliseconds, typically delivering 15-30 picoliters antibody solution or 3-30 pl BAC/mRNA solution. Due to the sticky nature of the antibody solution, we silanized all capillary tubes used for its injection, prior to pulling the capillary tubes into injection needles. The silanization consisted of soaking the

capillary tubes in 5% dichlorodimethylsilane (Lancaster) in chloroform for one hour, drying the tubes in a jet of air, soaking the tubes in acetone for two minutes, drying again, then baking in a 56 °C oven overnight²⁹.

After injection, the embryos were incubated at 15 °C in filtered seawater. Once they hatched, the embryos were transferred to round-bottom 96-well plates to be scored for motility. Immotile embryos readily sank to the bottom of their wells, and formed hexagonal close-packed arrays. Motile embryos (which presumably had not received an amount of antibody sufficient to eliminate cilia function completely) tended not to form such arrays, instead swimming or twitching slightly, and were excluded from subsequent imaging.

Microscopy

When placed on the bottom of a flat petri dish, embryos with immotile cilia still tend to roll slightly during the course of several minutes, likely due to convection currents in the surrounding seawater. To reduce this movement, we coated our dishes (Chambered #1.0 Borosilicate Coverglass System, Lab-Tek, catalog #155380) with protamine sulfate, or mounted embryos in agar tunnels³⁰.

Confocal imaging was performed on a Zeiss LSM 5 Exciter microscope, using a 63x C-Apochromat 1.2 NA W objective lens. To maintain 15 °C embryo temperature during imaging, we found that an objective-cooling collar (Bioptechs) supplied with chilled water was sufficient, cooling the coverglass chamber solely via the drop of immersion water. To prevent condensation from developing on the back

glass of the objective, we used a thermal isolator (Bioptechs) supplied with air regulated to 12 psig.

Green fluorescence (GFP, Dendra2) was excited at 488 nm (10% power of a 25 mW Ar laser) and detected through a 505-545 nm bandpass emission filter. Red fluorescence (H2B-mCherry) was excited at 543 nm (10% power of a 1 mW He/Ne laser) and detected through a 560 nm longpass emission filter. Cyan fluorescence (H2B-Cerulean) was excited at 405 nm (1% power of a 25 mW diode laser) and detected through a 505-530 nm bandpass emission filter. We typically imaged using a 6.4 μs pixel dwell time with 0.50 μm pixel size (256 x 256 pixel image size). The pinhole was set to 535 μm (4.75 Airy units in green channel, 4.32 Airy units in red channel, 4.85 Airy units in cyan channel) creating optical slices of <4.0 μm . Z-stacks were collected with an interval of 2.0 μm , with a total stack size of 100-120 μm .

Image analysis

Confocal time-lapse data were processed using the application Imaris (Bitplane). Raw fluorescence data were despeckled using a 3x3x1 median filter. Then the nuclear fluorescence signal (resulting from injected mRNA) was normalized over time to compensate for any photobleaching. Slight wobble and drift of the embryo were compensated for by recursive alignment^{31,32}. Individual nuclei were then tracked over time, first using the automated segmentation and tracking features of Imaris, then manually validated. The data in this paper were obtained from detailed imaging performed on nine different embryos. Only a representative fraction of these data could be included in the figures.

Acknowledgements We thank Julie Hahn for construction of the recombineered reporter BACs; Andy Ransick for help with agar tunnels; and Michael Liebling for help with software, including his RecursiveReg alignment plugin for Imaris. We are pleased to acknowledge Andy Ransick's perspicacious review of a draft of the manuscript. This work was supported by National Institutes of Health NRSA grant 5 T32 GM07616 (M.E.B.) and NIH grant HD37105 to E.H.D. and S.E.F.

Author Contributions The specific gastrula regulatory problem was formulated by I.S.P. and E.H.D.; S.E.F. provided technological input in respect to imaging technology; and M.E.B. invented the critical method for long term imaging of the embryos. M.E.B. executed all the actual experiments and carried out all the primary data analysis. M.E.B., I.S.P., E.H.D. and S.E.F. were all involved in interpretation, various aspects of experimental design, and preparation of the manuscript.

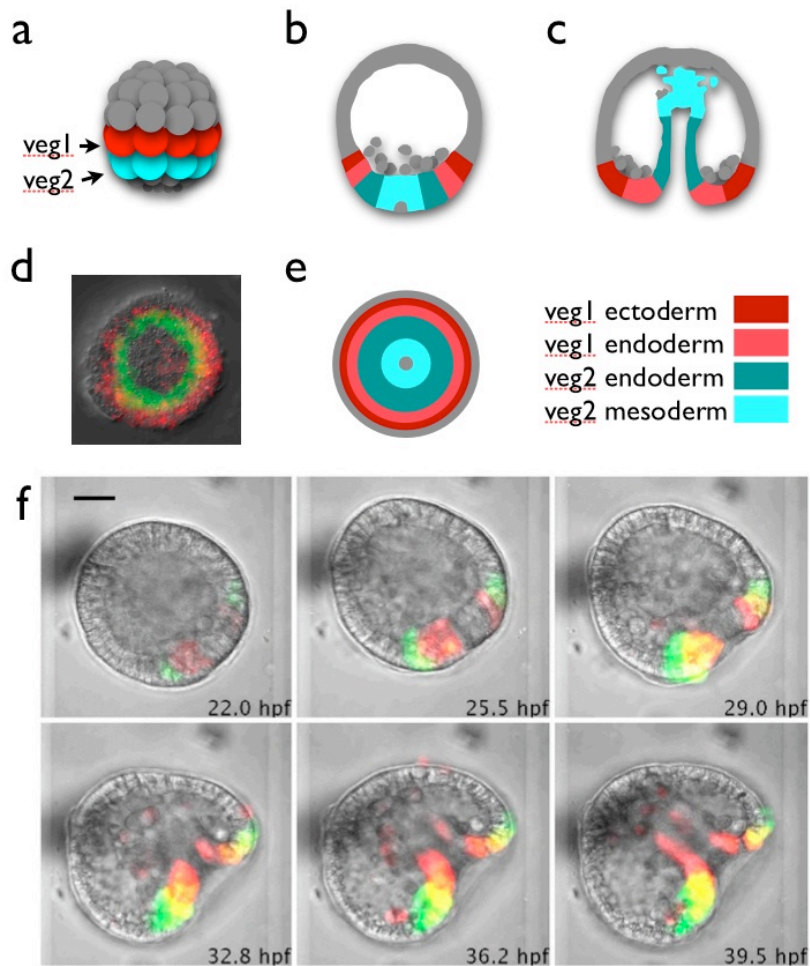


Figure 1 Vegetal lineages of the sea urchin embryo, and *in vivo* time-lapse imaging of gene expression in a single embryo during gastrulation. **a**, Sixth-cleavage embryo (~8 hpf), which has eight veg1 (red) and eight veg2 (blue) blastomeres. Cells of the animal half of the embryo (above the veg1 tier) and cells of the micromere lineages (at the vegetal pole of the embryo below the veg2 tier) are shown in gray. **b**, Mesenchyme-blastula stage embryo (~24 hpf), in which precocious ingressions of the skeletogenic mesenchyme cells (derived from the large micromeres) has occurred. Cells of the veg2 lineage (along with the eight small micromere descendants) form the vegetal plate of the embryo. The veg1 and veg2 lineages are shown subdivided based on their fates: veg1 ectoderm, dark red; veg1 endoderm, light red; veg2 endoderm, dark blue; veg2 mesoderm, light blue. **c**, Late-gastrula stage embryo (~40 hpf), color-coded as in (b). **d**, WMISH of a mesenchyme-blastula stage embryo showing mRNA expression of *foxa* (green) and *brachyury* (red), in vegetal view. **e**, Vegetal view of the embryo depicted in (b), showing the concentric arrangement of veg1 and veg2 lineages, with the small micromere descendants at the center. **f**, Time-lapse images of a sea urchin embryo expressing *foxa:RFP* (red) and *brachyury:GFP* (green) recombinereed BAC reporters, which mark the veg2 and veg1 territories, respectively. Yellow indicates overlapping expression of these two genes. The projection of fluorescence from a 20- μ m slab of confocal slices was superimposed over the transmitted-light image from a single focal depth to form each composite image. Scale bar, 20 μ m. hpf: hours post-fertilization. See also Supplementary Information, Video S2 online.

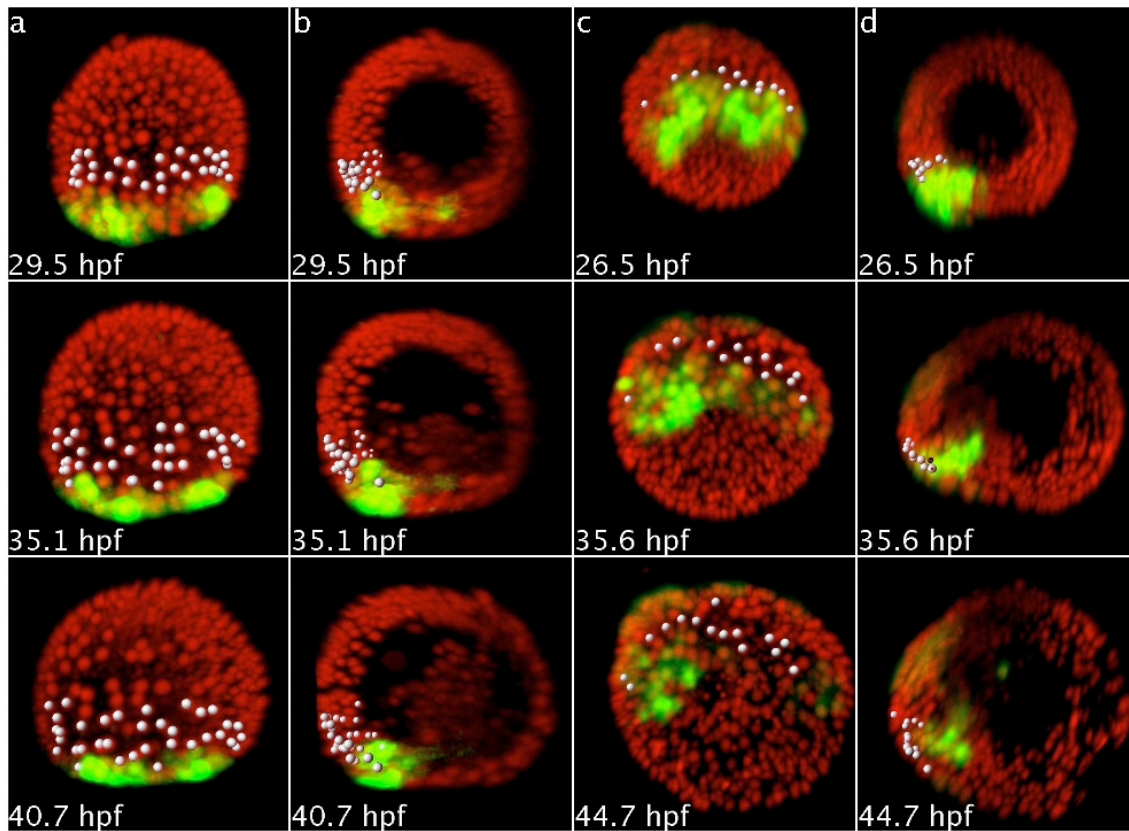


Figure 2 Cells outside the ring of *brachyury* expression prior to gastrulation do not contribute to the archenteron or to the blastopore during gastrulation. **a**, Time-lapse images of a sea urchin embryo expressing a *brachyury:GFP* BAC reporter in a background of H2B-mCherry expression, aboral view. White spots indicate nuclei of cells that are outside the ring of *brachyury* expression at the beginning of the time lapse, and that do not express GFP for the duration of the time lapse. In this embryo, mosaic incorporation of the *brachyury:GFP* reporter occurred in the aboral half of the embryo. The single row of cells separating the white tracked cells and the bright green GFP cells are also GFP positive, but only faintly so. **b**, Same embryo as in (a) but seen in a lateral view, with portions of the ectoderm computationally removed so the elongating archenteron is visible. **c**, Time-lapse images of an embryo in which mosaic incorporation of the *brachyury:GFP* reporter occurred in the oral half of the embryo. The view is oral-vegetal. **d**, Same embryo as in (c) but in lateral view. All images are maximum-intensity projections of confocal image stacks. The embryo is ~100 μm in diameter at these stages. See also Supplementary Information, Videos S3, S4, S5 and S6 online.

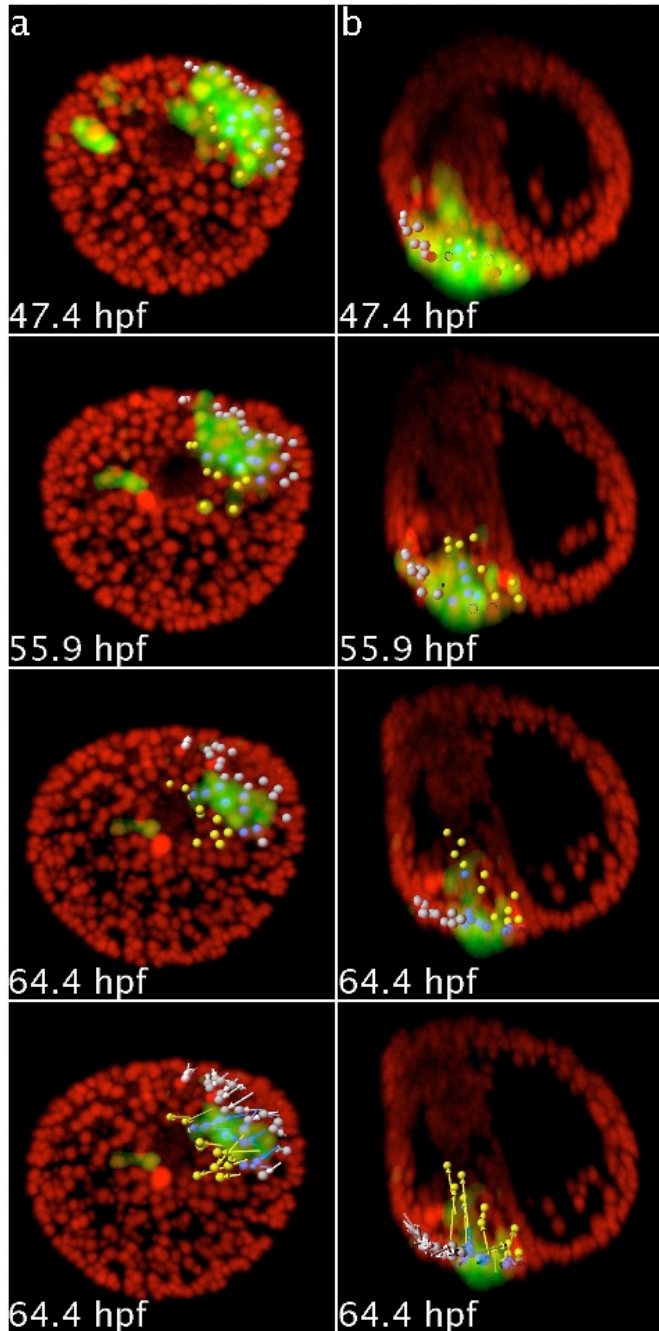


Figure 3 Cells outside the ring of *brachyury* expression prior to gastrulation do not contribute to the archenteron or to the blastopore by prism stage. **a**, Time-lapse images of a sea urchin embryo expressing a *brachyury:GFP* BAC reporter in a background of H2B-mCherry expression, vegetal view. White spots indicate nuclei of cells that are outside the ring of *brachyury* expression at the beginning of the time lapse, and that do not express GFP for the duration of the time lapse. Blue spots indicate cells expressing GFP throughout the time lapse. Yellow spots indicate cells that initially express GFP, but do not express it at the end of the time lapse (likely *veg2*-derived cells). Color-coded arrows indicate the net movement of each tracked cell. **b**, Same embryo as in (a) but seen in lateral view. See also Supplementary Information, Videos S7 and S8 online.

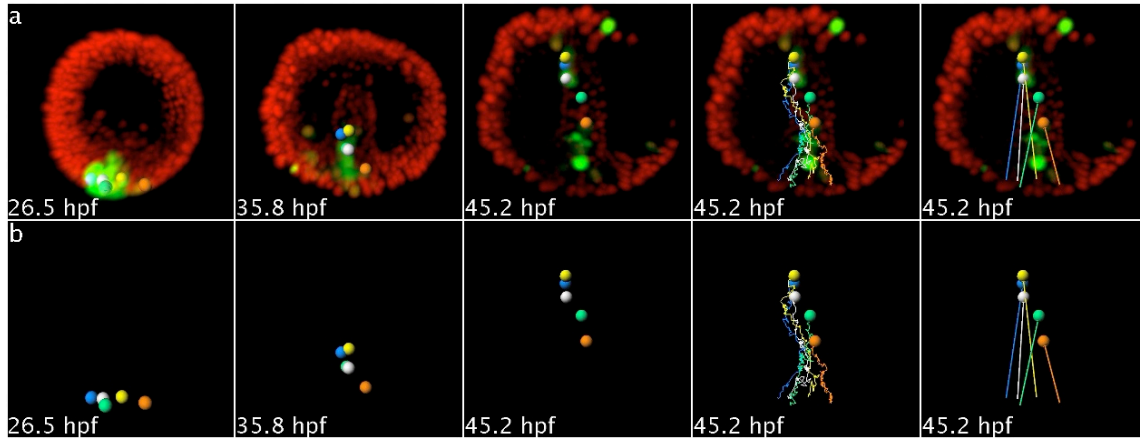


Figure 4 During gastrulation, cells expressing *foxa* form the anterior endoderm by local rearrangement. **a**, Time-lapse images of a sea urchin embryo expressing a *foxa:dendra2* BAC reporter in a background of H2B-mCherry expression, lateral view. Spots indicate nuclei of five cells expressing the reporter at the beginning of the time lapse. Color-coded lines indicate the trajectories of the five cells, as well as their net movement. **b**, Same view as in (a) but showing the tracked cells without the fluorescence channels. See also Supplementary Information, Videos S9 and S10 online.

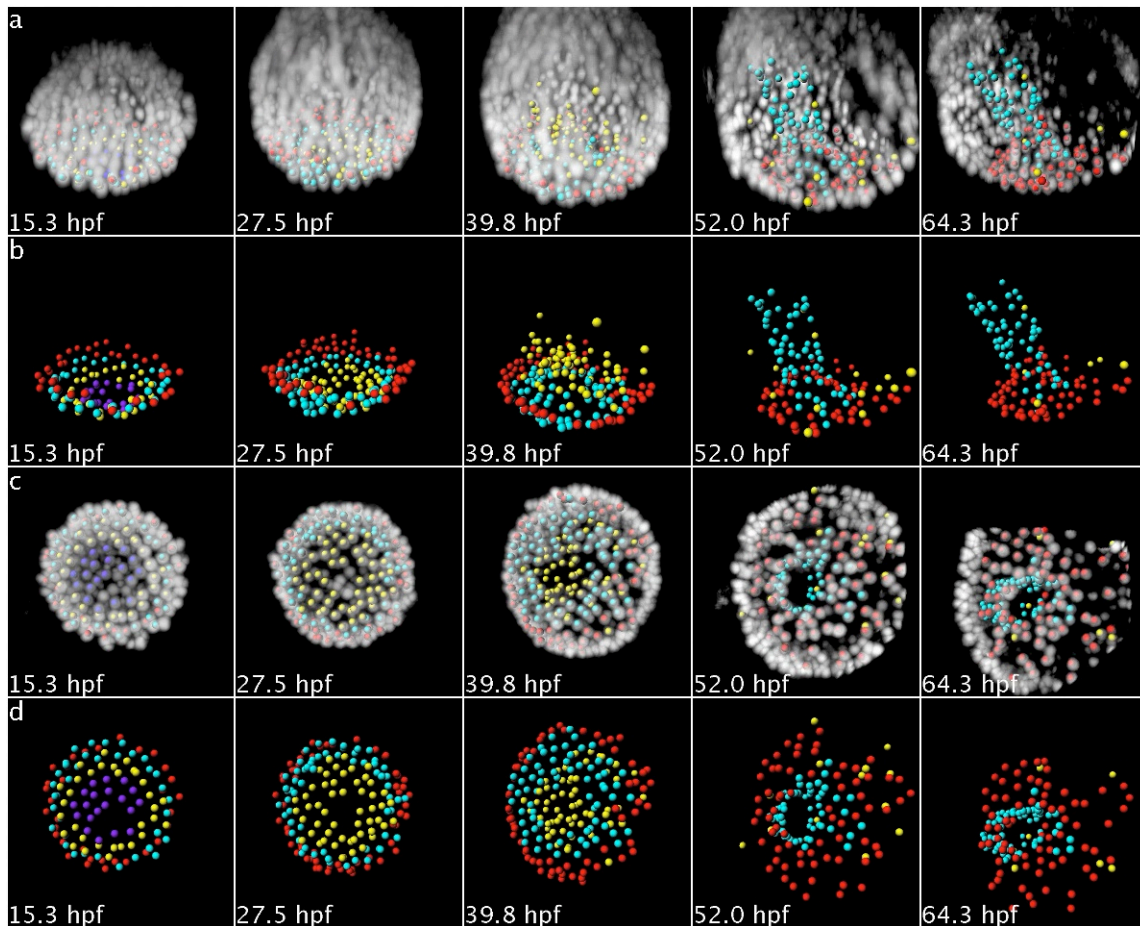


Figure 5 The cellular basis of gastrulation. **a**, Time-lapse images of a sea urchin embryo expressing H2B-mCherry (false colored white) in all cells, lateral view. **b**, Same view as in (a), but showing only the cells that were tracked, without the fluorescence channel. Purple, large-micromere descendants (skeletogenic mesenchyme cells); yellow, veg2 non-skeletogenic mesoderm; cyan, veg2 endoderm; red, veg1. Once they ingress from the vegetal pole, around 25 hpf, the skeletogenic mesenchyme cells were no longer tracked. Similarly, many of the non-skeletogenic mesoderm cells were not tracked for the entire time lapse, since the primary purpose of identifying them was to label the surrounding veg2 endoderm at the early stages. **c**, Same as (a), but vegetal view. **d**, Same as (c), but without the fluorescence channel. The concentric arrangement of lineages around the vegetal pole prior to gastrulation is evident. See also Supplementary Information, Videos S11, S12, S13 and S14 online.

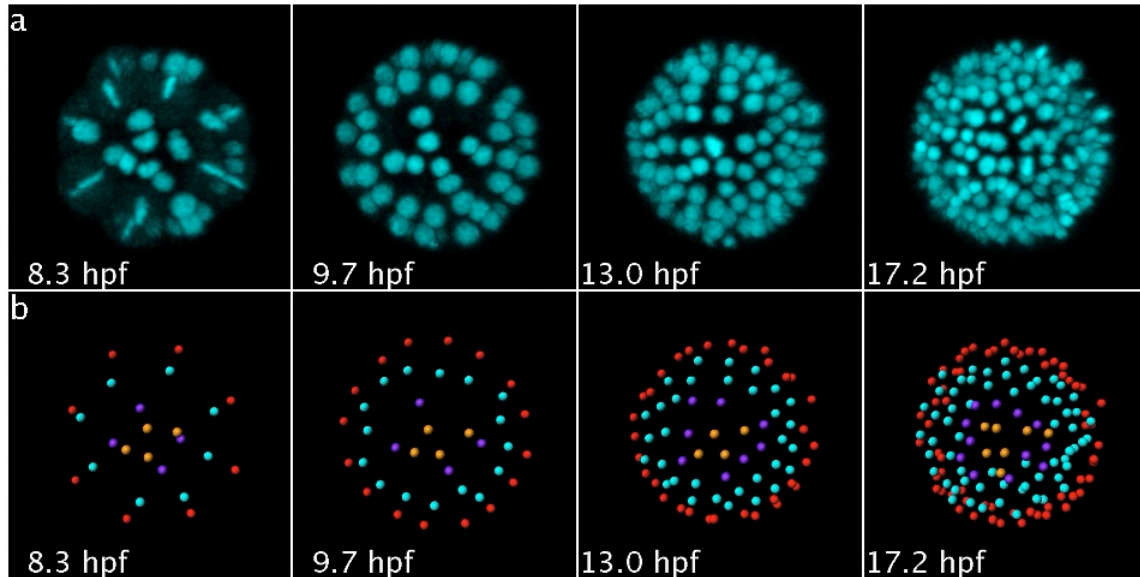


Figure 6 Vegetal-half lineages from sixth to ninth embryonic cleavages. **a**, Time-lapse images of a sea urchin embryo expressing H2B-Cerulean in all cells, vegetal view. **b**, Same view as in (a), showing the different lineages of the vegetal half of the embryo. After sixth cleavage (~ 7.5 hpf), the 56-cell embryo consists of four small micromeres (orange), four large micromeres (purple), eight veg2 blastomeres (cyan), eight veg1 blastomeres (red) and 32 animal-half blastomeres (not shown). Seventh cleavage (~ 9.7 hpf) doubles the number of cells in both the veg1 and veg2 rings, but in *S. purpuratus* the micromeres do not divide again until the veg1 and veg2 progeny undergo their next division, at the eighth embryonic cleavage (~ 13.0 hpf). Ninth cleavage (~ 17.2 hpf), less synchronized than prior cycles, results in approximately 64 veg1 and 64 veg2 blastomeres, about the time the embryo hatches from its fertilization envelope. See also Supplementary Information, Videos S15 and S16 online.

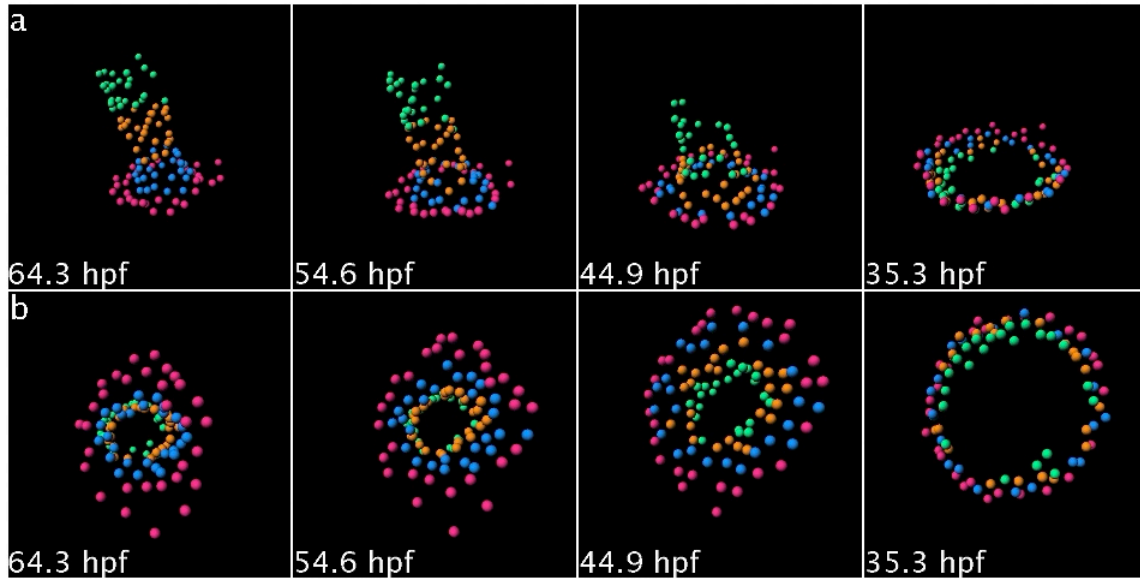


Figure 7 The ordering of concentric rings of cells is generally maintained during gastrulation, with some local mixing. **a**, Alternate color-coding of veg2 endodermal cells and veg1 cells of the time lapse shown in Fig. 5, lateral view. Cells were computationally color-coded based on their final location along or outside of the archenteron, then their developmental trajectories were followed in reverse to see where they originated prior to gastrulation. **b**, Same embryo as in (a), vegetal view. See also Supplementary Information, Videos S17, S18 and S19 online.

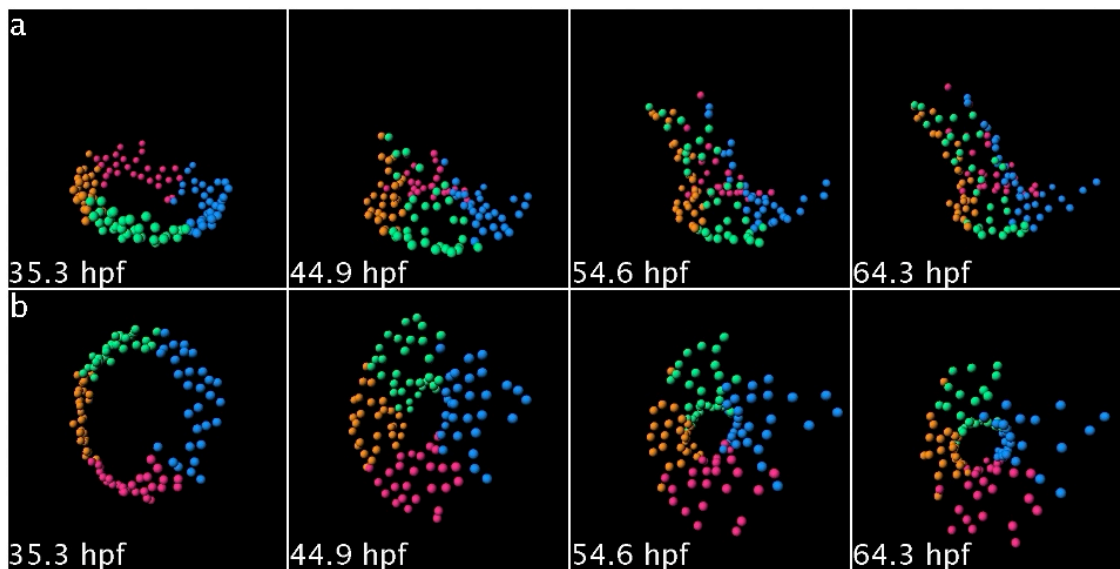


Figure 8 The ordering of circumferential quadrants of cells is generally maintained during gastrulation, with some local mixing. **a**, Alternate color-coding of veg2 endodermal cells and veg1 cells of the time lapse shown in Fig. 5, lateral view. Cells were computationally color-coded based on their location prior to gastrulation (35.3 hpf: oral, orange; aboral, blue; left, magenta; right, green), then their developmental trajectories were followed during gastrulation. **b**, Same embryo as in (a), vegetal view. See also Supplementary Information, Videos S20 and S21 online.

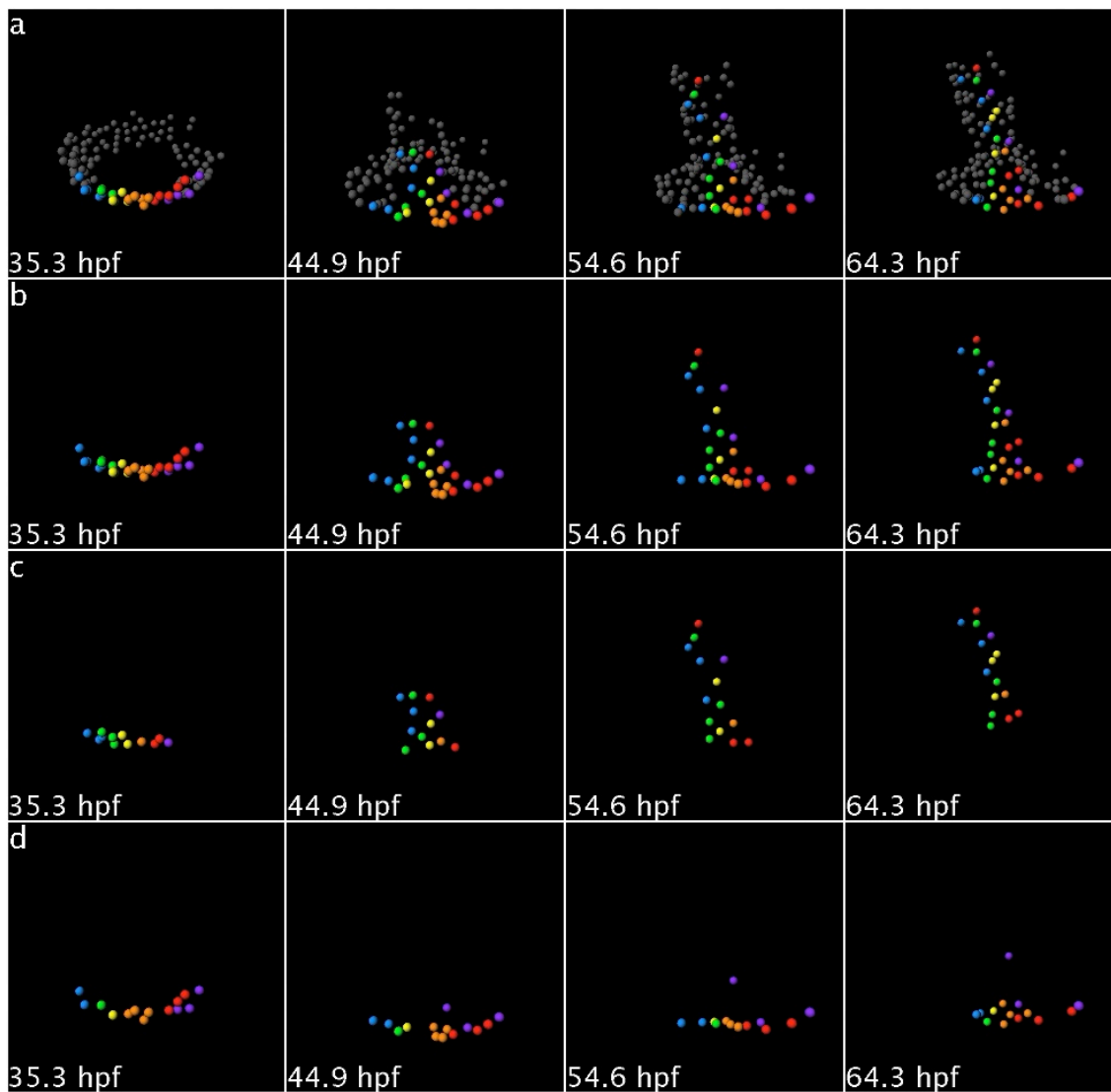


Figure 9 Veg2-derived cells form the archenteron by intercalative convergent extension, whereas veg1-derived cells form a coherent truncated cone encompassing the hindgut and blastopore. **a**, Alternate color-coding of veg2 endodermal cells and veg1 cells of the time lapse shown in Fig. 5, lateral view. Six radial stripes of cells, comprising one-quarter the circumference of the embryo, were computationally labeled (blue, green, yellow, orange, red, purple). Cells comprising the remaining circumference were labeled gray for clarity. **b**, Same view as in (a), but without displaying the gray cells, so that only the quadrant of archenteron formed by the rainbow-labeled cells is visible. **c**, Same view as in (b), but displaying only the veg2-derived cells. **d**, Same view as in (b), but displaying only the veg1-derived cells. See also Supplementary Information, Videos S22, S23, S24 and S25 online.

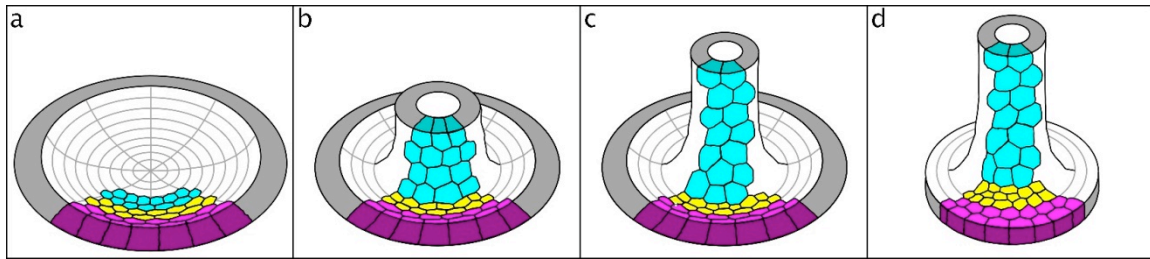


Figure 10 Model of gastrulation supported by our tracking experiments. **a**, Pregastrula stage, illustrating a quadrant of cells of the veg2 endoderm (cyan), veg1 endoderm (yellow) and veg1 ectoderm (magenta). Cells of the non-skeletogenic mesoderm territory, at the center of the vegetal plate, have been omitted for clarity. **b**, Mid-gastrula stage, showing intercalative convergent extension of the veg2 endoderm driven by the *foxa* regulatory state in these cells, while cells of the veg1 endoderm, under the control of the *brachyury* regulatory state, remain outside the forming archenteron. **c**, Late-gastrula stage, at which point veg2 endodermal cells have undergone further intercalative rearrangement to form the anterior endoderm, while veg1 endodermal cells remain in the blastopore area. **d**, Later still, the ring of veg1 endodermal cells constricts to form the definitive blastopore, the inner part of the ring tipping into the archenteron to form the hindgut. Veg1 ectodermal cells, outside the ring of *brachyury*-expressing veg1 endodermal cells at the pregastrula stage, never contribute to the archenteron. The quantity of cell division depicted is representative of that observed in our tracking experiments.

Supplementary Video S1

Brightfield time lapse of five embryos from the single-cell stage to hatched-blastula stage, at which point they hatch from their fertilization envelopes and begin to swim.

Supplementary Video S2

Video from which still frames were taken for Figure 1f. *In vivo* time-lapse imaging of gene expression during gastrulation in a single embryo.

Supplementary Video S3

Video from which still frames were taken for Figure 2a. Tracking of cells outside the vegetal ring of *brachyury* expression, aboral clone, aboral view.

Supplementary Video S4

Video from which still frames were taken for Figure 2b. Tracking of cells outside the vegetal ring of *brachyury* expression, aboral clone, lateral view.

Supplementary Video S5

Video from which still frames were taken for Figure 2c. Tracking of cells outside the vegetal ring of *brachyury* expression, oral clone, oral-vegetal view.

Supplementary Video S6

Video from which still frames were taken for Figure 2d. Tracking of cells outside the vegetal ring of *brachyury* expression, oral clone, lateral view.

Supplementary Video S7

Video from which still frames were taken for Figure 3a. Tracking of cells outside the vegetal ring of *brachyury* expression, later-stage embryo, vegetal view.

Supplementary Video S8

Video from which still frames were taken for Figure 3b. Tracking of cells outside the vegetal ring of *brachyury* expression, later-stage embryo, lateral view.

Supplementary Video S9

Video from which still frames were taken for Figure 4a. Rearrangement of cells expressing *foxa* during gastrulation. Lateral view including both fluorescence data and tracked nuclei.

Supplementary Video S10

Video from which still frames were taken for Figure 4b. Rearrangement of cells expressing *foxa* during gastrulation. Lateral view including only tracked nuclei.

Supplementary Video S11

Video from which still frames were taken for Figure 5a. Cellular movements during gastrulation. Lateral view including both fluorescence data and tracked nuclei.

Supplementary Video S12

Video from which still frames were taken for Figure 5b. Cellular movements during gastrulation. Lateral view including only tracked nuclei.

Supplementary Video S13

Video from which still frames were taken for Figure 5c. Cellular movements during gastrulation. Vegetal view including both fluorescence data and tracked nuclei.

Supplementary Video S14

Video from which still frames were taken for Figure 5d. Cellular movements during gastrulation. Vegetal view including only tracked nuclei.

Supplementary Video S15

Video from which still frames were taken for Supplementary Figure S1a. Vegetal-half lineages from sixth to ninth embryonic cleavages. Vegetal view of fluorescence data.

Supplementary Video S16

Video from which still frames were taken for Supplementary Figure S1b. Vegetal-half lineages from sixth to ninth embryonic cleavages. Vegetal view of tracked nuclei.

Supplementary Video S17

Video from which still frames were taken for Figure 6a. Ordering of concentric rings of cells during gastrulation. Lateral view of tracked nuclei, played in reverse developmental time.

Supplementary Video S18

Video from which still frames were taken for Figure 6b. Ordering of concentric rings of cells during gastrulation. Vegetal view of tracked nuclei, played in reverse developmental time.

Supplementary Video S19

Video from which still frames were taken for Figure 6b. Ordering of concentric rings of cells during gastrulation. Vegetal view of tracked nuclei, played in reverse developmental time. Slightly different viewing angle from Supplementary Video S18, to better show cellular arrangement prior to gastrulation.

Supplementary Video S20

Video from which still frames were taken for Supplementary Figure S2a. Ordering of circumferential quadrants of cells during gastrulation. Lateral view of tracked nuclei.

Supplementary Video S21

Video from which still frames were taken for Supplementary Figure S2b. Ordering of circumferential quadrants of cells during gastrulation. Vegetal view of tracked nuclei.

Supplementary Video S22

Video from which still frames were taken for Figure 7a. Intercalative rearrangement during gastrulation. Lateral view, all tracked veg2 endodermal and veg1 nuclei.

Supplementary Video S23

Video from which still frames were taken for Figure 7b. Intercalative rearrangement during gastrulation. Lateral view, one-quarter-circumference tracked veg2 endodermal and veg1 nuclei.

Supplementary Video S24

Video from which still frames were taken for Figure 7c. Intercalative rearrangement during gastrulation. Lateral view, one-quarter-circumference tracked veg2 endodermal nuclei.

Supplementary Video S25

Video from which still frames were taken for Figure 7d. Intercalative rearrangement during gastrulation. Lateral view, one-quarter-circumference tracked veg1 nuclei.

- 1 Dan, K. & Okazaki, K. Cyto-Embryological Studies of Sea Urchins .3. Role of the Secondary Mesenchyme Cells in the Formation of the Primitive Gut in Sea Urchin Larvae. *Biol Bull* **110**, 29-42 (1956).
- 2 Burke, R. D., Myers, R. L., Sexton, T. L. & Jackson, C. Cell Movements during the Initial Phase of Gastrulation in the Sea-Urchin Embryo. *Developmental Biology* **146**, 542-557 (1991).
- 3 Ettensohn, C. A. Primary Invagination of the Vegetal Plate during Sea-Urchin Gastrulation. *Am Zool* **24**, 571-588 (1984).
- 4 Hardin, J. The cellular basis of sea urchin gastrulation. *Curr Top Dev Biol* **33**, 159-262 (1996).
- 5 Peter, I. S. & Davidson, E. H. The endoderm gene regulatory network in sea urchin embryos up to mid-blastula stage. *Developmental Biology* **340**, 188-199, doi:Doi 10.1016/J.Ydbio.2009.10.037 (2010).
- 6 Davidson, E. H. *et al.* A provisional regulatory gene network for specification of endomesoderm in the sea urchin embryo. *Developmental Biology* **246**, 162-190 (2002).
- 7 Davidson, E. H. *et al.* A genomic regulatory network for development. *Science* **295**, 1669-1678 (2002).

- 8 Rast, J. P., Cameron, R. A., Poustka, A. J. & Davidson, E. H. brachyury target genes in the early sea urchin embryo isolated by differential macroarray screening. *Developmental Biology* **246**, 191-208, doi:Doi 10.1006/Dbio.2002.0654 (2002).
- 9 Beane, W. S., Gross, J. M. & McClay, D. R. RhoA regulates initiation of invagination, but not convergent extension, during sea urchin gastrulation. *Developmental Biology* **292**, 213-225, doi:Doi 10.1016/J.Ydbio.2005.12.031 (2006).
- 10 Peter, I. S. & Davidson, E. H. Modularity and design principles in the sea urchin embryo gene regulatory network. *Febs Lett* **583**, 3948-3958, doi:Doi 10.1016/J.Febslet.2009.11.060 (2009).
- 11 Gross, J. M. & McClay, D. R. The role of Brachyury (T) during gastrulation movements in the sea urchin *Lytechinus variegatus*. *Developmental Biology* **239**, 132-147 (2001).
- 12 Nakajima, Y. & Burke, R. D. The initial phase of gastrulation in sea urchins is accompanied by the formation of bottle cells. *Developmental Biology* **179**, 436-446 (1996).

- 13 Hardin, J. Local Shifts in Position and Polarized Motility Drive Cell Rearrangement during Sea-Urchin Gastrulation. *Developmental Biology* **136**, 430-445 (1989).
- 14 Ransick, A. & Davidson, E. H. Late specification of veg(1) lineages to endodermal fate in the sea urchin embryo. *Developmental Biology* **195**, 38-48 (1998).
- 15 Piston, D. W., Summers, R. G., Knobel, S. M. & Morrill, J. B. Characterization of involution during sea urchin gastrulation using two-photon excited photorelease and confocal microscopy. *Microsc Microanal* **4**, 404-414 (1998).
- 16 Logan, C. Y. & McClay, D. R. The allocation of early blastomeres to the ectoderm and endoderm is variable in the sea urchin embryo. *Development* **124**, 2213-2223 (1997).
- 17 Martins, G. G., Summers, R. G. & Morrill, J. B. Cells are added to the archenteron during and following secondary invagination in the sea urchin *Lytechinus variegatus*. *Developmental Biology* **198**, 330-342 (1998).
- 18 Etensohn, C. A. Gastrulation in the Sea-Urchin Embryo Is Accompanied by the Rearrangement of Invaginating Epithelial-Cells. *Developmental Biology* **112**, 383-390 (1985).

- 19 Keller, R., Davidson, L. A. & Shook, D. R. How we are shaped: The biomechanics of gastrulation. *Differentiation* **71**, 171-205 (2003).
- 20 Stephens, L., Hardin, J., Keller, R. & Wilt, F. The Effects of Aphidicolin on Morphogenesis and Differentiation in the Sea-Urchin Embryo. *Developmental Biology* **118**, 64-69 (1986).
- 21 Morris, R. L. & Scholey, J. M. Heterotrimeric kinesin-II is required for the assembly of motile 9+2 ciliary axonemes on sea urchin embryos. *Journal Of Cell Biology* **138**, 1009-1022 (1997).
- 22 Takeda, S. *et al.* Kinesin superfamily protein 3 (KIF3) motor transports fodrin-associating vesicles important for neurite building. *Journal Of Cell Biology* **148**, 1255-1265 (2000).
- 23 Oliveri, P., Walton, K. D., Davidson, E. H. & McClay, D. R. Repression of mesodermal fate by foxa, a key endoderm regulator of the sea urchin embryo. *Development* **133**, 4173-4181, doi:Doi 10.1242/Dev.02577 (2006).
- 24 Croce, J., Lhomond, G. & Gache, C. Expression pattern of Brachyury in the embryo of the sea urchin *Paracentrotus lividus*. *Dev Genes Evol* **211**, 617-619, doi:Doi 10.1007/S00427-001-0200-5 (2001).

- 25 Livant, D. L., Houghevans, B. R., Moore, J. G., Britten, R. J. & Davidson, E. H. Differential Stability of Expression of Similarly Specified Endogenous and Exogenous Genes in the Sea-Urchin Embryo. *Development* **113**, 385-398 (1991).
- 26 Ruffins, S. W. & Ettensohn, C. A. A fate map of the vegetal plate of the sea urchin (*Lytechinus variegatus*) mesenchyme blastula. *Development* **122**, 253-263 (1996).
- 27 Davidson, E. H. *The regulatory genome : gene regulatory networks in development and evolution*. (Academic, 2006).
- 28 Damle, S., Hanser, B., Davidson, E. H. & Fraser, S. E. Confocal quantification of cis-regulatory reporter gene expression in living sea urchin. *Developmental Biology* **299**, 543-550, doi:Doi 10.1016/J.Ydbio.2006.06.016 (2006).
- 29 Morris, R. L. *et al.* Microinjection methods for analyzing the functions of kinesins in early embryos. *Methods Mol Biol* **164**, 163-172 (2001).
- 30 Ransick, A. & Davidson, E. H. Micromeres Are Required for Normal Vegetal Plate Specification in Sea-Urchin Embryos. *Development* **121**, 3215-3222 (1995).

- 31 Vermot, J., Fraser, S. E. & Liebling, M. Fast fluorescence microscopy for imaging the dynamics of embryonic development. *Hfsp J* **2**, 143-155, doi:Doi 10.2976/1.2907579 (2008).
- 32 Thevenaz, P., Ruttimann, U. E. & Unser, M. A pyramid approach to subpixel registration based on intensity. *Ieee T Image Process* **7**, 27-41 (1998).

Chapter 3: Conclusions

This thesis demonstrates a method for imaging individual sea urchin embryos for several hours or even days of development, and for subsequently tracking individual cells of the embryo as it undergoes morphogenesis. Prior to this work, observation of the dynamic behavior of individual cells of the sea urchin embryo was temporally restricted to the range of minutes to a few hours^{1,2}. To circumvent this limitation, the constraint of cellular resolution was often relaxed, with researchers using lipophilic dyes to track clonal populations of cells in individual embryos^{3,4}. Alternatively, to achieve cellular resolution, a series of embryos could be fixed at several developmental stages, then compared across time^{5,6}. Conclusions drawn from such series provide valuable insight, but are tempered by the caveat that a different individual embryo is assayed at each developmental time point, making it difficult to connect individual cells across time. The method described in this thesis overcomes these difficulties, allowing individual cells to be followed for periods of time encompassing major morphogenetic events. Combined with the injection of recombinered BAC reporters, this method allows us to relate cell behavior and lineage to regulatory state, and thus provides a powerful tool for studying the genetic basis for lineage specification and morphogenesis in the sea urchin embryo.

By employing this method, I have shown that cells outside the vegetal ring of *brachyury* expression prior to gastrulation do not contribute to the archenteron, or to the blastopore, during gastrulation. Instead, they remain in an almost fixed position. Moreover, cells outside the *brachyury* ring prior to gastrulation do not turn on *brachyury* expression, even as some move by one or two cell diameters toward the

vegetal pole. My results do not support the hypothesis of a highly dynamic regulatory situation in which cells move into the ring of *brachyury* expression, turn on *brachyury* themselves, then turn off *brachyury* as they enter the archenteron⁶. Instead, my results show that the fixed location of the *brachyury* ring during gastrulation is due to the relatively fixed location of veg1 endodermal cells expressing this gene.

Using the 4D imaging and tracking method on cells of the veg2 lineage revealed that they undergo a dramatic rearrangement via intercalative convergent extension. Rearrangement of veg2 cells had been deduced previously by examining cross sections of fixed embryos at different developmental stages⁵. Direct observation of rearrangement, however, had only been performed during a brief period of archenteron elongation in the cidaroid urchin, *Eucidaris tribuloides*¹. Because of the short duration of this observation, and because at least one of *E. tribuloides*' cell lineages behaves morphogenetically differently from that of euechinoid urchins, the rearrangement I observed during the entirety of gastrulation in *Strongylocentrotus purpuratus* is novel and important. Moreover, by combining a marker of cellular regulatory state with lineage-based cell tracking, my results support a model of gastrulation that connects regulatory state to morphogenetic function. Specifically, in this model, the *foxa* regulatory state in cells of the veg2 endoderm causes them to rearrange by intercalation, thus driving the elongation of the archenteron. By contrast, the *brachyury* regulatory state in cells of the veg1 endoderm prevents them from substantial rearrangement. This leads to the prediction that there will be different sets of cytoskeletal and motility genes expressed in these two endodermal lineages. Discovering the gene regulatory

connections between high-level transcription factors (such as *foxa* and *brachyury*), and the downstream genes responsible for cell morphology and behavior, will be crucial for our understanding of the genetic basis of gastrulation.

References

- 1 Hardin, J. Local Shifts in Position and Polarized Motility Drive Cell Rearrangement during Sea-Urchin Gastrulation. *Developmental Biology* **136**, 430-445 (1989).
- 2 Miller, J., Fraser, S. E. & McClay, D. Dynamics of Thin Filopodia during Sea-Urchin Gastrulation. *Development* **121**, 2501-2511 (1995).
- 3 Logan, C. Y. & McClay, D. R. The allocation of early blastomeres to the ectoderm and endoderm is variable in the sea urchin embryo. *Development* **124**, 2213-2223 (1997).
- 4 Ransick, A. & Davidson, E. H. Late specification of veg(1) lineages to endodermal fate in the sea urchin embryo. *Developmental Biology* **195**, 38-48 (1998).
- 5 Etensohn, C. A. Gastrulation in the Sea-Urchin Embryo Is Accompanied by the Rearrangement of Invaginating Epithelial-Cells. *Developmental Biology* **112**, 383-390 (1985).
- 6 Gross, J. M. & McClay, D. R. The role of Brachyury (T) during gastrulation movements in the sea urchin *Lytechinus variegatus*. *Developmental Biology* **239**, 132-147 (2001).

